Atmospheric
Chemistry
and Physics
Discussions

Open Access

Supplement of

Chemical composition, microstructure, and hygroscopic properties of aerosol particles at the Zotino Tall Tower Observatory (ZOTTO), Siberia, during a summer campaign

E. F. Mikhailov et al.

Correspondence to: E. F. Mikhailov (eugene.mikhailov@spbu.ru)

Supplementary material

S.1 Impactor characterization experiment

The experimental setup used for the characterization of the MOUDI impactor stages is shown schematically in Fig. S1. The apparatus consists of two major components: the particle generation system and the particle sampling and monitoring system. An aqueous solution of ammonium sulfate (AS) was used to generate submicron (0.1-1 µm) and supermicron (1-20 µm) particles using a constant output atomizer (3076 TSI Inc.) and vibrating orifice aerosol generator (3450 TSI Inc.), respectively. The solution droplets generated by the collision atomizer were dried using a self-made silica gel diffusion dryer (SDD) with an aerosol residence time of ~7 s. For both aerosol generators the residual relative humidity of the dry aerosol flow was <10% RH. The 3450 TSI and 3076 TSI neutralizers were used to stabilize the particles' electrostatic charge. A stainless tank (20 L) fitted with inlet and outlet valves was used to separate impaction and measurement modes. The electrical mobility diameters and aerodynamic diameters of the particles were measured by a scanning mobility particle sizer (SMPS; Model 3936, TSI Inc.) and an aerodynamic particle sizer (APS; Model 3321, TSI Inc.), respectively. The SMPS and APS size spectra were measured separately for stages I and II. The collection efficiency for a given particle size bin and for each impaction stage was calculated as the normalized difference between the input and penetrated particle concentration. Particle concentrations were measured seven times for each two-minutes scan. The reproducibility of the last three scans were within ±5%. For the SMPS data, each particle size interval was converted from the mobility equivalent diameter to the aerodynamic diameter using the AS particle density (1.77 g/cm^3) and the shape factor of 1(Khlystov et al., 2004).
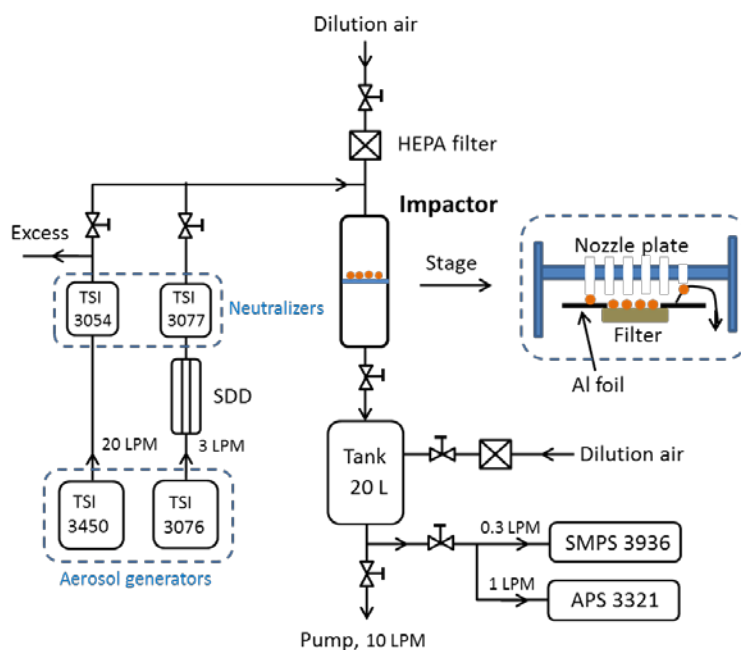

Figure S1. Schematic design of calibration test setup for particles in 0.1 – 20 µm size range.

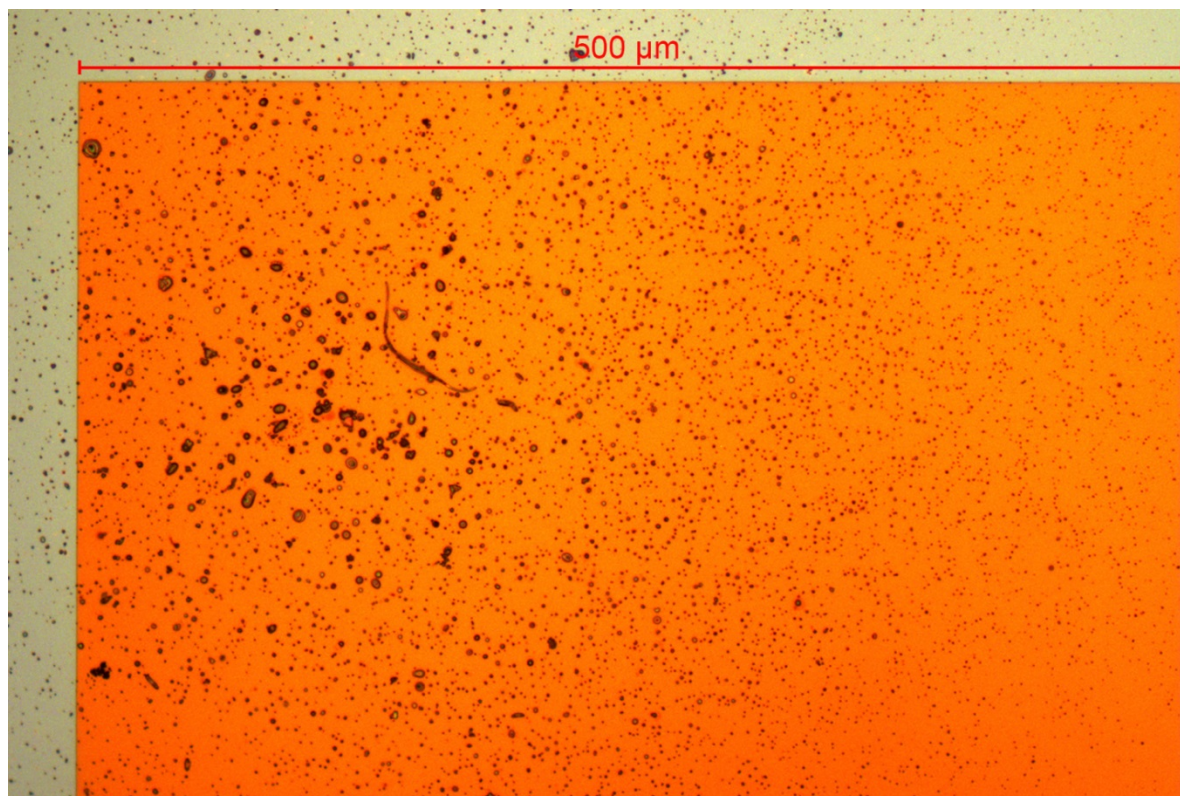**S2. The light microscopy and STXM-NEXAFS images of the ZOTTO aerosol samples**

Figure S2.1 Light microscopy image of the STXM sample taken on June 15. Image shows impaction spot with larger CM particles (> 1 µm) in upper left corner. The majority of particles belongs to AM size range (0.3 – 1 µm). AM particles are spread around impaction spot center and show gradient of particle sizes with smallest particles being deposited in periphery of impaction spot.
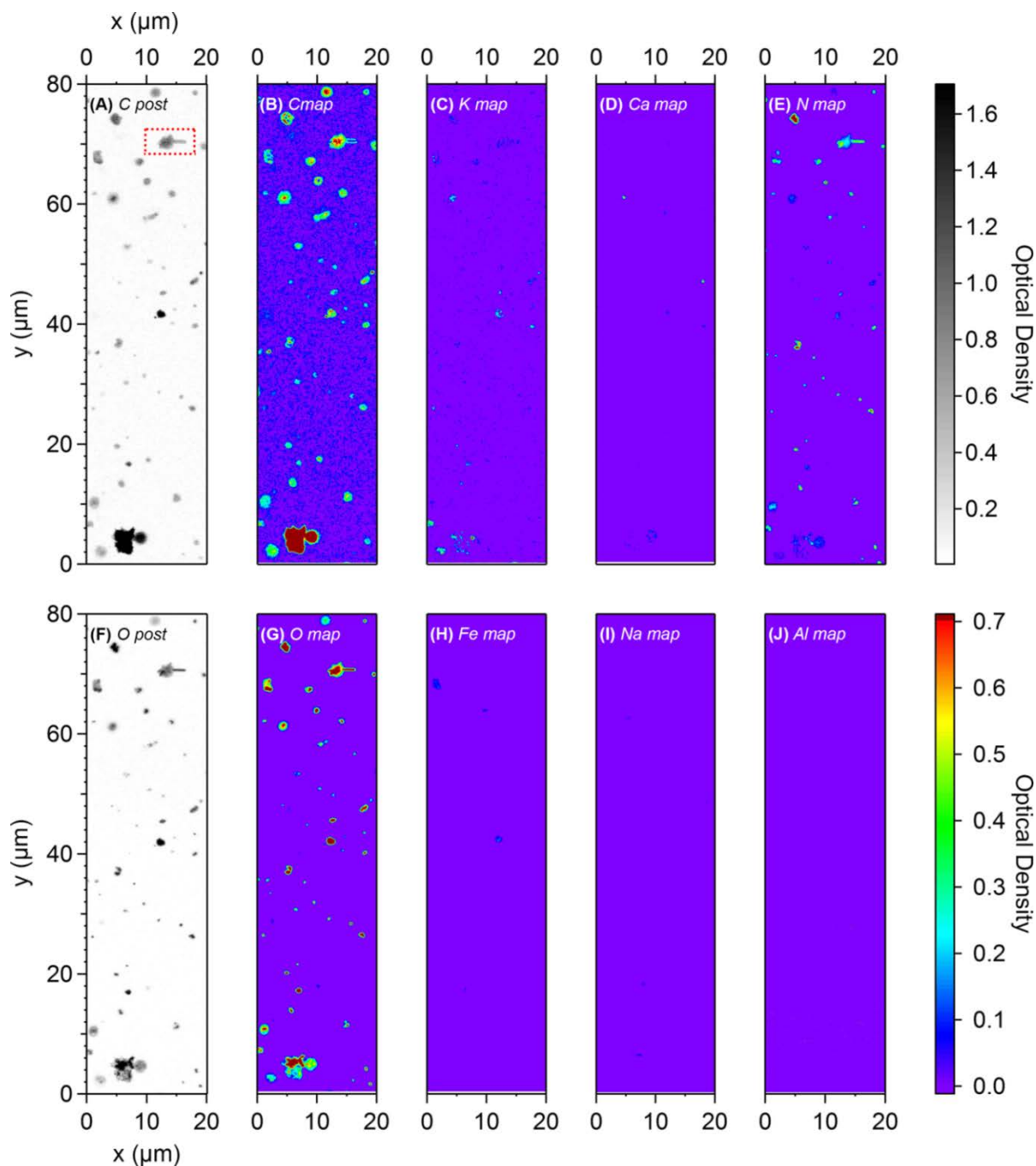
Figure S2.2 STXM overview images and maps for various elements showing characteristic region on aerosol sample taken on June 15. (**A** and **F**) show carbon and oxygen post-edge images with all particles in the field of view. (**B**-**E** and **G**-**J**) show elemental maps for various elements. Overview maps show that the clear majority of particles is strongly absorbing at the characteristic energies of N as well as O and shows moderate absorption for C. Few particles also absorb at the K and/or Ca edges. However, no x-ray absorption has been found for iron (Fe) and aluminum (Al), which would be typical components of mineral dust particles. The absence of irregular shaped particles further emphasizes that mineral dust does not play a significant role in the sampling period of this study. Axes display image dimensions in μm. Optical density is unified for all STXM images (black-white code; OD range 0 - 1.7) and unified for all elemental maps (color code; OD range 0 - 0.7). Red box in (**A**) marks particle with beam damage (horizontal line) due to refocussing.
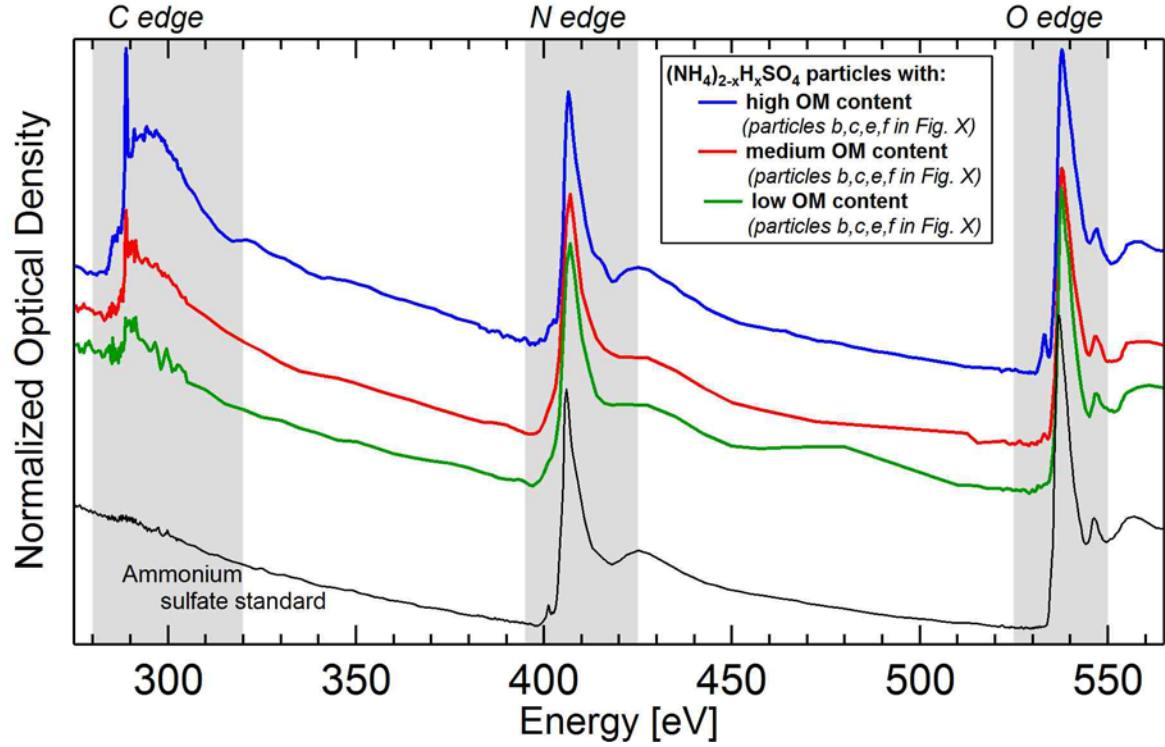
Figure S2.3 X-ray absorption spectra across C, N, and O edges of ZOTTO aerosol samples. Spectral shape at the nitrogen edge indicates ammonium as dominant nitrogen species. Spectral structure at the oxygen edge is typical for sulfate-rich particles. Colored traces represent the spectra of particles that are shown in the elemental maps in Fig. 5 and 6. For comparison, CNO spectrum for standard ammonium sulfate is shown. Spectra confirm that ammonium sulfate particles are predominant with variable amounts of organic material.

S3 Conversion of the organic carbon to organic matter concentrations.

The following relations were used to convert the measured organic carbon (OC), water soluble organic carbon (WSOC), and water insoluble organic carbon (WIOC) into organic matter (OM), water soluble (WSOM), and water insoluble (WIOM) organic matter, respectively:

$$\frac{WSOM}{OM} = \frac{cf_1 WSOC}{cf_1 WSOC + cf_2 WIOC} = cf_{1,2}\frac{WSOC}{OC}, \tag{S3.1}$$

where cf_1 and cf_2 are the conversion factors of WSOC to WSOM and WINOC to WIOM, respectively; $cf_{1,2}$ is the conversion factor of the WSOC/OC to WSOM/OM ratio. From Eq.(S3.1) follows:

$$cf_{1,2} = \frac{cf_1}{\left(cf_1\beta + cf_2\left(1-\beta\right)\right)}; \qquad \beta = \frac{WSOC}{OC} \quad . \tag{S3.2}$$

For total PM the conversion factors are $cf_1 = 1.97\pm0.35$ and $cf_2 = 1.40\pm0.14$, which were obtained as weighted average values reported for rural conditions by Lathem et al. (2013), Finessi et al. (2013),

Yttri et al. (2007), and Turpin and Lim (2001). Inserting cf_1 and cf_2 values and experimentally determined $\beta = 0.67 \pm 0.06$ and OC (Section 4.1) into Eq. (S3.2) we obtain $cf_{1,2}=1.10 \pm 0.22$. Thus, for total PM the estimated WSOM/OM ratio is 0.74 ± 0.22.

To reconstruct the WSOM and OM in the coarse mode fraction of the ZOTTO samples we used Timonen et al.'s (2008) size-segregated MOUDI measurements in the boreal region, which were determined for the summer season (June, July) and include long-range transported aerosols, local small-scale wood combustion, and aerosols in air masses from clean arctic and marine areas. We took the averaged WSOM/PM value obtained for the coarse mode and combined it with the OM and PM content in ZOTTO sample (Table 2). The calculated WSOM/OM ratio for the CM is 0.21 ± 0.07. Using this ratio and the following relation

$$\frac{WSOM}{OM} = \frac{WSOM(AM) + WSOM(CM)}{OM(AM) + OM(CM)} = 0.74 \qquad (S3.3)$$

we estimate WSOM in the accumulation mode. The calculated concentrations of WSOM and WIOM (= OM-WSOM) in the AM and CM fractions are given in Table 2.

References

Finessi, E., Decesari, S., Paglione, M., Giulianelli, L., Carbone, C., Gilardoni, S., Fuzzi, S., Saarikoski, S., Raatikainen, T., Hillamo, R., Allan, J., Mentel, Th. F, Tiitta, P., Laaksonen, A., Petäjä, T., Kulmala, M., Worsnop, D. R., and Facchini, M. C.: Determination of the biogenic secondary organic aerosol fraction in the boreal forest by NMR spectroscopy, Atmos. Chem. Phys., 12, 941–959, 2012

Khlystov, A., Stanier, C., and Pandis S. N.: An algorithm for combining electrical mobility and aerodynamic size distributions data when measuring ambient aerosol, Aeros.Sci. Technol., 38, 229-238, 2004.

Lathem, T. L., Beyersdorf, A. J., Thornhill, K. L., Winstead, E. L., Cubison, M. J., Hecobian A., Jimenez, J. L., Weber, R. J., Anderson, B. E., and Nenes, A.: Analysis of CCN activity of Arctic aerosol and Canadian biomass burning during summer 2008, Atmos. Chem. Phys., 13, 2735–2756, 2013.

Turpin, B. J., and Lim, H. J.: Species Contributions to PM2.5 Mass Concentrations: Revisiting Common Assumptions for Estimating Organic Mass, Species Contributions to PM2.5 Mass Concentrations: Revisiting Common Assumptions for Estimating Organic Mass, Aerosl Sci. Techol. 35, 602–610, 2001.

Yttri, K. E. Aas, W., Bjerke, A., Cape, J. N., Cavalli, F., Ceburnis, D., Dye, C., Emblico, L., Facchini, M. C., Forster, C., Hanssen, J. E., Hansson, H. C., Jennings, S. G., Maenhaut, W., Putaud, J. P., and Tørseth, K.: Elemental and organic carbon in PM10: a one year measurement campaign within the European Monitoring and Evaluation Programme EMEP, Atmos. Chem. Phys., 7, 5711–5725, 2007.